OBJECT-BASED DUNE MAPPING AND CHARACTERIZATION ON MARS: DATA COMPARISON AND ACCURACY ASSESSMENT. David A. Vaz[1,2], Pedro T.K. Sarmento[1,3], L. K. Fenton[4], M. T. Barata[1], T.I. Michaels[4], [1]CITEUC - Centre for Earth and Space Research of the University of Coimbra, Observatório Geofísico e Astronómico da UC, Almas de Freire, 3040-004 Coimbra, Portugal (davidvaz@uc.pt), [2]CERENA, Instituto Superior Técnico, Lisboa, Portugal, [3]ESAC - European Space and Astronomy Center, Madrid, Spain, [4]Carl Sagan Center, SETI Institute, 189 N Bernardo Ave, Mountain View, CA 94043, USA.

Introduction: The nearly global coverage of the CTX imagery, at spatial resolutions <10 m/pixel, enables a detailed analysis of dune fields on Mars. Such a large amount of data will be used in the upcoming years to study aeolian processes and to update existing dune catalogs, such as the Mars Global Digital Dune Database [1, 2]. Unless this analysis is totally or partially automated, a considerable human effort must be employed, since it basically relies on manual photointerpretation of orbital imagery.

By adapting the same generic procedure developed for the mapping of aeolian ripples from HiRISE data [3], we have explored the possibility of automated dune pattern characterization [4]. Here we will present the first results, including a preliminary validation of the technique by comparing the results with photointerpretations of the dune fields located in Gale crater and Ganges Chasma.

Data and methodologies: Using ISIS (Integrated Software for Imagers and Spectrometers) we have produced geometrically controlled CTX mosaics with a spatial resolution of 6 and 7 m/pixel, for the Gale Crater and Ganges Chasma areas respectively.

The automated mapping procedure follows the same type of object-based approach described in [3], and it includes: 1) segmentation from the CTX mosaic of the linear bright and dark ridges that can correspond to dune morphologies; 2) vectorization and characterization of the mapped objects (geometric, textural, morphometric and spectral descriptors are computed for each object); 3) supervised classification using neural networks, in order to exclude non-aeolian objects and segment the population of objects that correspond to slipfaces.

In this report we will discuss the accuracy rate of the implemented supervised classification, which constitutes the basis for future analysis. This processing step is fundamental, since it guarantees the segmentation of the objects that represent dune morphologies such as crests or slipfaces.

The obtained results are compared quantitatively and qualitatively with photointerpretations of the same areas. For this purpose we use the same mapping outputs previously discussed in [5] for the Ganges area. The objective is to assess the limitations of the methodology.

Results and discussion: Object descriptors are the input parameters for the classification process. A training dataset with three classes was created, allowing the segmentation of objects that do not correspond to dune morphologies (corresponding in most cases to bedrock features), slipface traces and other dune morphologies (a class that includes dune limbs, ridges, crests, etc.). Figure 1b shows an example of this training dataset, which represents 15% of the total mapped objects. Globally for the two areas, the computed overall accuracy was 94%, with a *k* index of 0.7. These values indicate a significant degree of agreement between the photointerpretations and the mapped objects.

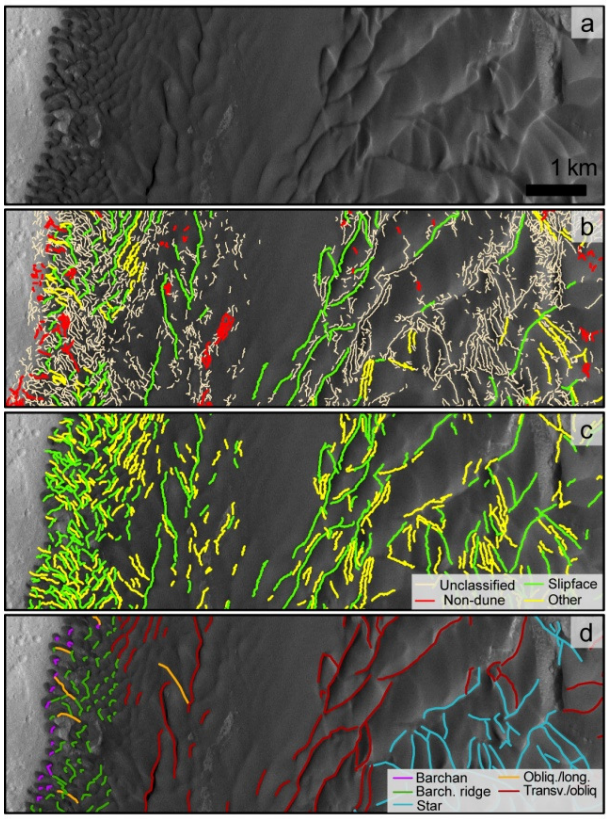

Figure 1 – Classification of the mapped objects, example from the Gale Crater area. a) CTX mosaic; b) mapped objects where the colored lines represent the training dataset; c) results of the supervised classification; d) photointerpreted dataset obtained by visual inspection and manual mapping of the dune morphologies (different classes represent the inferred dune types).

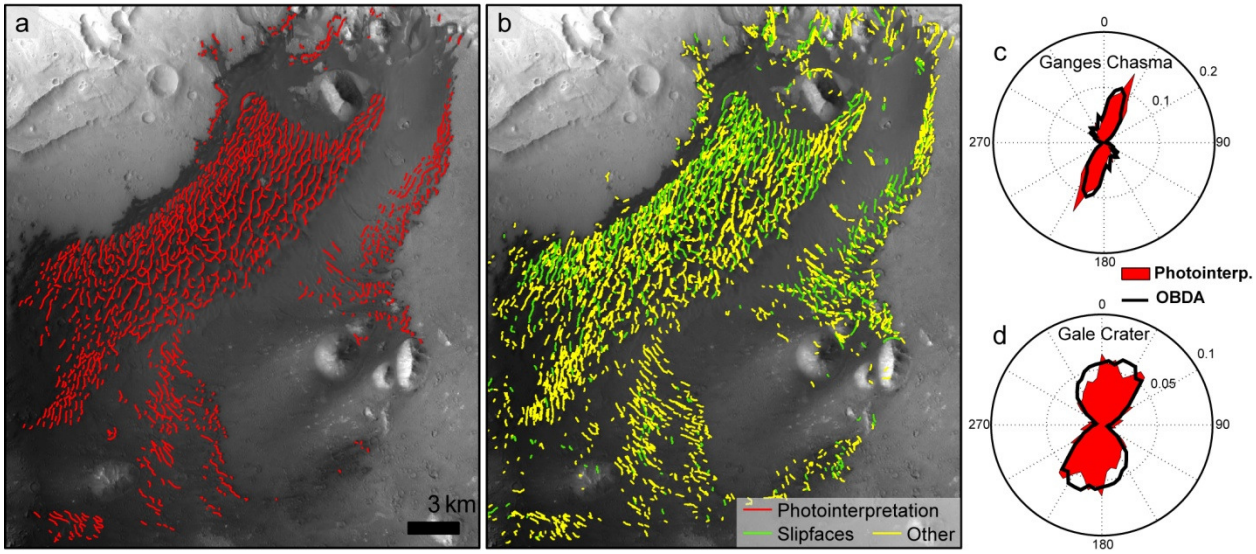

Figure 2 – Mapping results for the Ganges Chasma area and comparison of the circular distributions for the two areas. a) photointerpreted dune morphologies [5]; b) features automatically mapped; c and d) global length-weighted circular distributions for the photointerpreted and automatically derived datasets, note the good agreement between the obtained circular distributions.

Figures 2c and 2d show the global length-weighted circular distributions for the photointerpretations and also for the mapped dune morphologies. The good agreement between the circular distributions for both areas is evident. The angular differences in the trend of the mean axis computed between the two datasets are 5.2º and 4.6º, for Ganges and Gale respectively.

Qualitatively, the similarities in the mapping results are remarkable: compare figures 1c and 1d and 2a and 2b. Since the procedure is tuned to recognize all linear bright/dark regions on the image, it produces better results for larger linear features. Thus, small barchans dunes, which usually present small slipfaces, are not always correctly mapped (Fig, 1). For this dune type, barchans horns and lateral limbs are preferentially mapped. Because they are composed of larger scale linear features, barchanoid ridges, transverse and star dunes are better represented.

Conclusion and future perspectives: The supervised classification which enables the elimination of non-dune morphologies/objects is highly accurate and produces outputs that in qualitative terms are in agreement with the photointerpretations. At a regional level the circular distributions and the average axis of the mapped objects are highly correlated with the results obtained by photointerpretation.

We are currently evaluating the pattern differences at a local level, by implementing a zonal analysis and comparison of the mapped features. This is implemented by creating a sampling grid that is used to integrate the dune pattern characteristics locally. This enables a local quantitative comparison of the mapping results, and a simple integration of these results with mesoscale atmospheric model output.

In summary, we have shown that meaningful dune pattern characterization can be automatically performed for large areas using CTX image mosaics. A more detailed quantitative analysis of the results must still be performed. However, either integrated on a fully automated or semi-automated processing pipeline, the presented approach is potentially useful to implement a new data-driven wide survey of dune fields on Mars. This future survey would probably include automated morphological classification of the dune types and prediction of the sediment transport trends, using the mapped objects as inputs.

References: [1] Hayward R. K., et al. (2007). *Journal of Geophysical Research: Planets,* Vol. 112 (E11),E11007. [2] Hayward R. K., et al. (2014). *Icarus,* Vol. 230,38-46. [3] Vaz D. A. and S. Silvestro (2014). *Icarus,* Vol. 230,151-161. [4] Sarmento P. T. K., et al. (2014) Automated Dune Field Mapping from CTX Imagery, *45th LPSC*, #1777. [5] Fenton L. K., et al. (2014). *Icarus,* Vol. 230,47-63.

Acknowledgements: This work was supported by FCT (Fundação para a Ciência e a Tecnologia) with the grant FRH/BPD/72371/2010 and the contracts PEst-OE/CTE/UI0611/2012-CGUC and PTDC/CTE-SPA/117786/2010.